

Spatial and spectral filtering of supercontinuum emission generated in microstructure fibres

A.B. Fedotov, Ping Zhou, Yu.N. Kondrat'ev, S.N. Bagayev, V.S. Shevandin, K.V. Dukel'skii, A.V. Khokhlov, V.B. Smirnov, A.P. Tarasevitch, D. von der Linde, A.M. Zheltikov

Abstract. The mode structure of supercontinuum emission generated by femtosecond pulses of Ti:sapphire laser radiation in microstructure fibres is studied. The long-wavelength (720–900 nm) and visible (400–600 nm) parts of supercontinuum are shown to be emitted in spectrally separable isolated spatial modes. These spectrally sliced single modes of supercontinuum emission possess a high spatial quality, verified by efficient nonlinear-optical frequency conversion.

Keywords: microstructure fibres, nonlinear optics, supercontinuum.

1. Introduction

Supercontinuum (SC) generation in microstructure (MS) fibres [1–7] has been shown recently to offer several practical and elegant solutions to the problems of high-precision measurements [8–10], optical coherence tomography [11], short-pulse generation [12], and creation of new sources for spectroscopic studies. Due to the high degree of light-field confinement in the core of MS fibres [13] and the possibility to tailor the dispersion of guided modes [14], SC generation can be observed in such fibres with low-power femtosecond and even picosecond [2] laser pulses, suggesting the way to create compact and convenient broadband radiation sources for numerous applications.

Spectroscopic, tomographic, and metrological applications require the generation of reproducible supercontinua with stable temporal and spectral parameters, as well as with a high spatial mode quality. In many practically important situations, high efficiencies of supercontinuum generation

can be achieved due to multimode phase matching of four-wave mixing (FWM) processes contributing to spectral superbroadening. Supercontinuum can be emitted in several spatial modes under these conditions.

In this paper, we propose and experimentally implement a method for the spatial and spectral filtering of supercontinuum emission from a microstructure fibre. Physically, the possibility of such filtering of supercontinuum emission is based on the fact that the mismatch of propagation constants related to different waveguide modes increases with a decrease in the fibre core diameter. This observation brings us to the idea of using microstructure fibres with a small core diameter for supercontinuum generation in the regime when four-wave mixing processes contributing to SC generation are phase-matched only for one guided mode of SC emission at each frequency within each spectral region of SC emission (or at least within some of these spectral regions).

We have fabricated and studied fibres allowing this regime of SC emission to be implemented. The results of our experimental studies demonstrate the possibility of separating isolated spatial modes of SC emission generated in our MS fibres within different spectral ranges. The proposed method of filtering of single modes of SC emission provides a high quality of spatial distribution of SC emission intensity, ensuring a high efficiency of further nonlinear-optical frequency conversion of broad spectral slices of SC emission mixed with the fundamental radiation of a Ti:sapphire laser in a nonlinear crystal.

2. Experimental

To perform experiments on supercontinuum generation, we designed and fabricated a family of microstructure optical fibres with a cladding consisting of one, two, and more hexagonal cycles of air holes and additional light field localisation achieved due to a system of auxiliary air holes of smaller diameter (Fig 1). The architecture of microstructure fibres employed in these experiments is a result of joint work of M.V. Lomonosov Moscow State University and S.I. Vavilov State Optical Institute. The fibres were fabricated at S.I. Vavilov State Optical Institute using the technique similar to that described earlier in [15, 16].

In contrast to the standard procedure, however, a set of optical fibres with different diameters was used as the initial preform instead of a system of identical capillaries. In particular, a preform with a central part consisting of a fibre with a smaller diameter surrounded by six capillaries was employed to fabricate the basis fibre of this family – a

A.B. Fedotov, A.M. Zheltikov Department of Physics, M.V. Lomonosov Moscow State University, Vorob'evy gory, 119992 Moscow, Russia; e-mail: zheltikov@top.phys.msu.su;

Ping Zhou, A.P. Tarasevitch, D. von der Linde Institut für Laser- und Plasmaphysik, Universität Essen, D-45117 Essen, Germany;

Yu.N. Kondrat'ev, V.S. Shevandin, K.V. Dukel'skii, A.V. Khokhlov S.I. Vavilov State Optical Institute, All-Russian Scientific Center, Birzhevaya lin. 16, 199034 St. Petersburg, Russia;

S.N. Bagayev Institute of Laser Physics, Siberian Branch, Russian Academy of Sciences, prosp. akad. Lavrent'eva 13/3, 630090 Novosibirsk, Russia;

V.B. Smirnov Russian Center of Laser Physics, St. Petersburg State University, Peterhof, 198504 St. Petersburg, Russia

Received Received 17 May 2002

Kvantovaya Elektronika 32 (9) 828–832 (2002)

Translated by A.M. Zheltikov

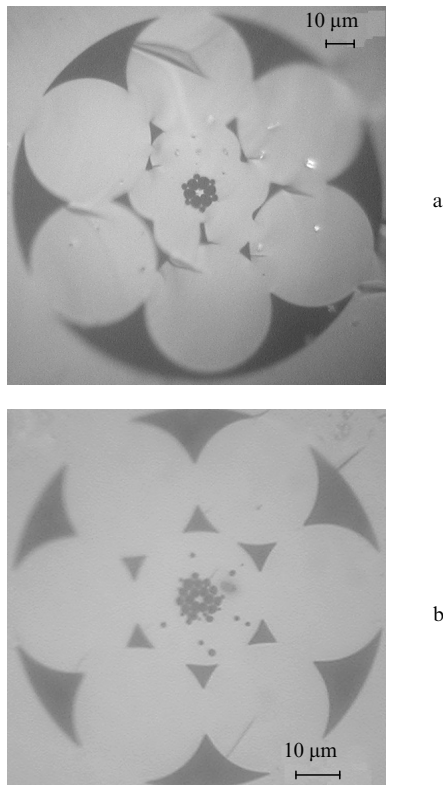


Figure 1. Microscope cross-sectional images of microstructure fibres: (a) a fibre with a single hexagonal cycle of air holes around the fibre core with a diameter of 2 μm and (b) a fibre with two hexagonal cycles of air holes around the fibre core with a diameter of 2 μm .

fibre with a single hexagonal cycle of holes around the fibre core (Fig. 1a). The fabrication of such a fibre with a minimal-microstructure cladding was earlier reported in [17].

The possibility to vary the spatial scale of the structure was built into the fibre fabrication procedure. The minimal core diameter in microstructure fibres employed in our experiments was 1 μm . Air holes provide a high refractive index step between the core and the cladding (Fig. 1). An additional light field localisation in the fibre core and lowering of optical losses are achieved due to the system of auxiliary air holes of smaller diameter, which increase the refractive index step between the core and the cladding and prevent the light field from leaking into the outer, fused silica part of the cladding (this effect can be seen in Fig. 2, which displays an image of a Ti:sapphire laser radiation intensity distribution measured at the output end of the fibre). The fibre with such a geometry is a basis fibre for the created family of fibres since the cladding of this fibre has a minimal number of holes (a single cycle of holes, plus auxiliary holes, improving light-field confinement in the fibre core).

To fabricate fibres with a more complicated structure, we modified the preform. In a microstructure fibre shown in Fig. 1b, the fused silica core is surrounded with two cycles of air holes and a system of smaller auxiliary holes, improving light-field confinement in the fibre core. The increase in the number of cycles of air holes around the fibre core reduces the magnitude of fibre losses. Optical losses have been determined for microstructure fibres of this type from the results of measurement [18] performed on $\sim 100\text{-m}$

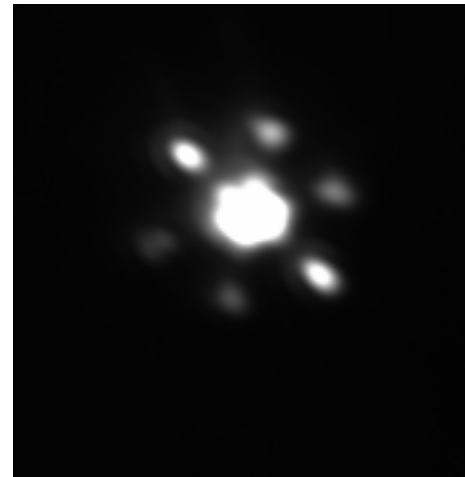


Figure 2. Transverse intensity distribution of Ti:sapphire laser radiation at the output end of a microstructure fibre with a single hexagonal cycle of air holes around the fibre core with a diameter of 2 μm in the low-power-pump no-supercontinuum-emission regime.

MS-fibre segments. The magnitude of optical losses was estimated to be 2–3 dB m^{-1} for fibres with a single hexagonal cycle of air holes in the cladding and 0.4–0.5 dB m^{-1} for fibres with two cycles of air holes.

Spectral broadening and supercontinuum generation in the created MS fibres were studied in our experiments with the use of femtosecond pulses produced by a Ti:sapphire laser system. This laser system included a Ti:sapphire master oscillator and a regenerative amplifier and was capable of generating 40-fs pulses of 800-nm radiation with the energy up to 0.2 mJ per pulse and a repetition rate of 1 kHz. Experiments were performed with fibre samples with a length of 4–200 cm. The laser beam was focused on the entrance face of a fibre sample, placed on a three-dimensional translation stage, with a microobjective (Fig. 3). Radiation coming out of the fibre was collimated with an identical microobjective and was split into two beams. One of these beams was delivered to a spectrograph, while the other one was used to visualise the transverse intensity distribution in the emission coming out of the MS fibre by imaging the output end of the fibre onto a CCD camera.

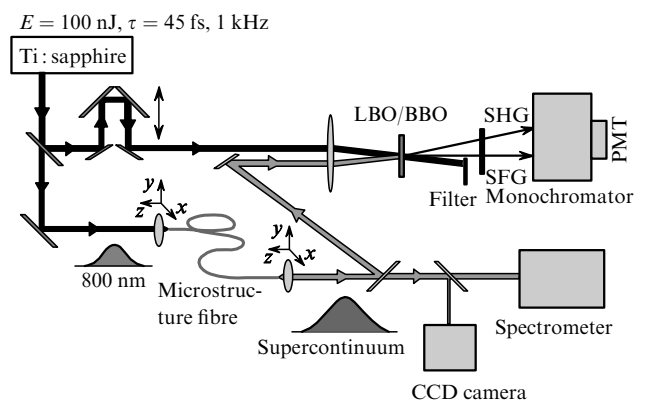


Figure 3. Scheme of the experimental setup for studying supercontinuum generation in microstructure fibres: SFG, the signal resulting from sum-frequency generation in the nonlinear crystal; SHG, the signal of second-harmonic generation; PMT, photoelectric multiplier.

3. The mode structure of supercontinuum emission

Propagation of femtosecond laser pulses through an MS fibre was accompanied by a considerable spectral broadening of these pulses. With only a few nanojoules of Ti:sapphire laser radiation coupled into an MS fibre sample with a length of several centimetres, we observed the generation of SC emission with a spectral bandwidth exceeding an octave. Fig. 4 shows typical spectra of supercontinuum generated by 40-fs pulses with an energy of 2 nJ (dotted curve) and 3 nJ (solid curve) in a 1.5-m MS fibre with a single ring of air holes around the fibre core and a core diameter of 3 μm .

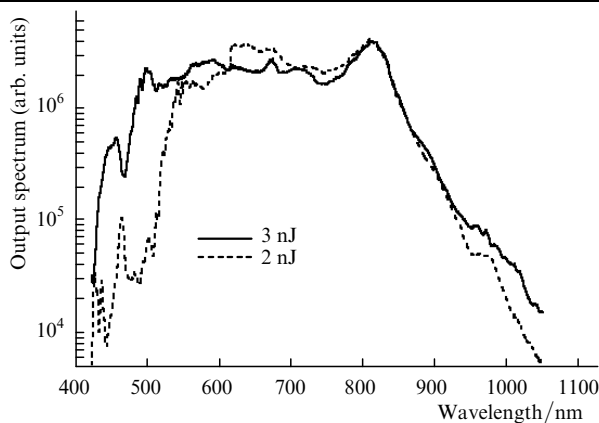


Figure 4. Spectra of SC emission generated by 40-fs pulses with an energy of 2 nJ (dotted curve) and 3 nJ (solid curve) in a 1.5-m MS fibre with a single ring of air holes around the fibre core (Fig. 1a) and a core diameter of 3 μm .

Fig. 2 displays the transverse intensity distribution of pump radiation at the output end of the fibre in the regime of low-power pump, when no SC is generated. The transverse structure of the guided mode of pump radiation, as can be seen from this image, features a sixfold rotational symmetry, which is also characteristic of the fibre structure. Supercontinuum emission was generally produced in the multimode regime in our experiments. However, we were able to filter isolated spatial modes for different spectral ranges of supercontinuum emission using a set of colour-glass filters. Figs 5a–5c present typical results of such experiments performed for an SC generated in a 1.5-m-long MS fibre with a single ring of air holes around the fibre core with a core diameter of 3 μm . The transverse intensity distribution of SC emission measured with a filter providing maximum transmission within the range of 720–900 nm (Fig. 5a) has a bell-like shape, displaying a single maximum on the beam axis. The visible part of SC emission (400–600 nm), on the other hand, has a doughnut-like spatial mode structure (Fig. 5b) under the same experimental conditions.

With a slight variation in the initial conditions of mode excitation at the input end of the MS fibre, this doughnut mode was transformed into a more complicated, two-lobe pattern shown in Fig. 5c. Both the doughnut-like mode of Fig. 5b and the two-lobe mode of Fig. 5c remained reproducible and stable and were observed for MS fibres with lengths ranging from several centimetres up to 2 m. Apparently, because of the poorer spatial overlapping

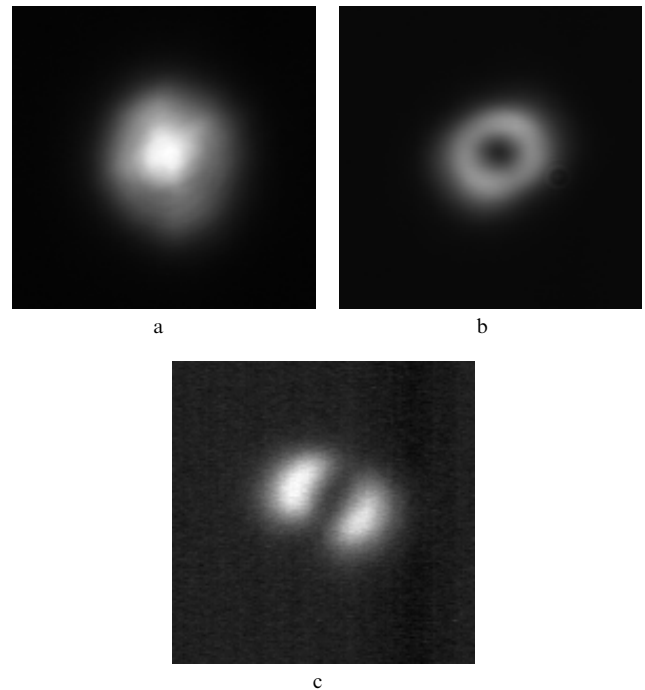


Figure 5. Transverse intensity distributions of SC emission generated in a 1.5-m-long MS fibre with a single ring of air holes around the fibre core with a core diameter of 3 μm measured within the spectral range of (a) 720–900 and (b, c) 400–600 nm. With a variation in the initial conditions at the input end of the fibre, a doughnut mode of the visible part of SC emission (b) tends to transform into a two-lobe mode (c).

between the pump beam and the two-lobe mode, the short-wavelength part of SC emission in the case of the two-lobe mode was much less intense than in the case of the doughnut mode.

Variations in the spatial distribution of SC intensity observed in our experiments indicate changes in multimode phase matching for four-wave mixing processes contributing to spectral superbroadening within different frequency ranges. Our experimental measurements performed for microstructure fibres with a core diameter of 3 μm also show that a certain spatial mode of the SC signal is predominantly phase-matched within each of the studied spectral ranges. This circumstance allows isolated spatial modes to be separated by spectrally slicing supercontinuum emission.

Four-wave mixing processes contributing to SC generation may be related to nonlinear-optical interactions of spectral components of frequency combs produced by mode-locked femtosecond lasers or may involve new frequency components resulting from stimulated Raman scattering or parametric wave-mixing processes. In the former case, multimode phase matching considered in this paper do not deteriorate the quality of SC emission considered from the viewpoint of metrological, spectroscopic, and biomedical applications (phase distribution, however, remains pretty much uncontrolled). In the latter case, multimode phase matching may lead to the generation of SC emission inapplicable for high-precision measurements. It will be shown below, however, that SC emission generated in this regime may possess a sufficiently high spectral and spatial quality, which makes this broadband emission an excellent tool for numerous spectroscopic applications.

4. Nonlinear-optical frequency conversion of spectrally sliced supercontinuum emission and cross-correlation measurements

Frequency convertibility of spectrally sliced supercontinuum is an important criterion of the quality of spatial modes of SC emission. Based on this criterion, we may also judge whether SC emission generated in MS fibres and spectrally sliced with the use of the above-described technique can be employed in practice for spectroscopic studies and pump–supercontinuum probe measurements.

With these circumstances in mind, we experimentally assessed the efficiency of nonlinear-optical frequency conversion for spectrally sliced spatial modes of SC emission produced in an MS fibre. The sum-frequency signal was produced in our experiments by mixing different parts of SC emission with the fundamental radiation of the above-described Ti:sapphire laser in a 100- μm -thick LBO crystal. Fig. 6 presents the results of these measurements performed with the use of the long-wavelength part (720–900 nm) of SC emission (the spectrum of this radiation is shown by curve (1) in panel (a) of Fig. 6) mixed with the fundamental radiation of the Ti:sapphire laser in the LBO crystal in the noncollinear geometry of sum-frequency generation (SFG). The broadband sum-frequency signal was produced within the spectral range from 370 up to 430 nm in the direction determined by phase-matching conditions [see diagram (I) in Fig. 6]. This geometry of sum-frequency generation allowed the efficiency of frequency conversion of about 0.1% to be achieved. We observed also collinear second-harmonic generation (SHG) using the long-wavelength part

of SC emission as a pump [see diagram (II) in Fig. 6]. The efficiency of this second-harmonic generation process under our experimental conditions was more than an order of magnitude lower than the efficiency of noncollinear sum-frequency generation (the relative efficiencies of SFG and SHG processes are shown on the left-hand side of Fig. 6).

Sum-frequency and second-harmonic generation experiments performed with spectrally sliced SC emission allow also the characteristic pulse duration to be estimated for different parts of SC emission. Panel (b) of Fig. 6 presents the results of such cross-correlation experiments, where the intensity of the sum-frequency signal was measured as a function of the delay time between the fundamental radiation pulse of the Ti:sapphire laser and the broadband emission pulse coming out of the fibre and passing through a set of optical filters. Cross-correlation traces measured with the use of this approach were compared with the results of cross-correlation measurements performed in the same geometry for low-intensity Ti:sapphire laser pulses transmitted through the MS fibre with virtually no or very weak spectral broadening [the spectrum of this signal is shown by line (2) in panel (a) of Fig. 6]. The cross-correlation trace measured for the broadband signal of spectrally sliced supercontinuum [curve (3) in panel (b) of Fig. 6] was much broader than the cross-correlation trace measured for the signal with virtually no or very weak spectral broadening [curve (4) in panel (b) of Fig. 6]. This comparison shows that different spectral components emitted as a part of supercontinuum are characterised by different delay times. This effect is associated with the dispersion properties of MS-fibre-guided modes and can be employed to temporally and spatially resolve different frequency components in pump supercontinuum probe experiments.

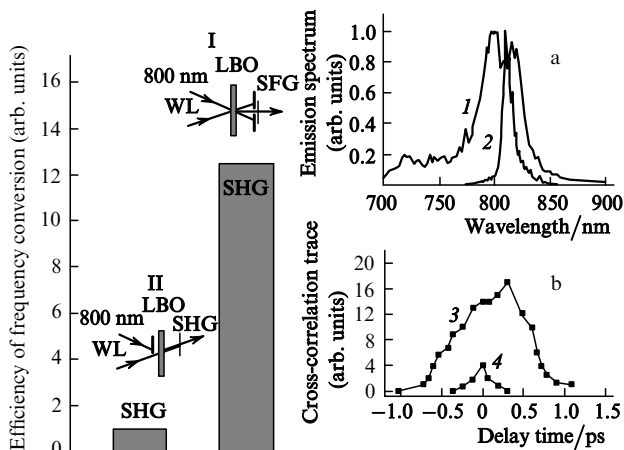


Figure 6. Nonlinear-optical frequency conversion of spectrally sliced white light (WL) and cross-correlation measurements. (a) The spectrum of supercontinuum emission produced within the range of wavelengths from 720 up to 900 nm in a microstructure fibre with a single ring of holes around the fibre core, a core diameter of 3 μm , and the length of 1.5 m (curve 1) and the spectrum of low-intensity Ti:sapphire laser pulses transmitted through the same microstructure fibre with virtually no or very weak spectral broadening (curve 2). (b) Cross-correlation traces for a pulse of the 720–900-nm spectral slice of supercontinuum (curve 3) and a weakly broadened low-intensity Ti:sapphire laser pulses transmitted through the same microstructure fibre with virtually no or very weak spectral broadening (curve 4). Beam diagrams of (I) noncollinear sum-frequency generation (SFG) and (II) collinear second-harmonic generation (SHG) are also shown. The heights of the vertical bars represent the relative efficiencies of the SFG and SHG processes.

5. Conclusions

Thus, we proposed and experimentally implemented the method of spatial filtering and spectral slicing of supercontinuum emission produced in microstructure fibres. The basic physical effect behind our method of spatial and spectral filtering of SC emission is associated with the increase in the separation between the propagation constants corresponding to adjacent guided modes with a decrease in the fibre core diameter. Microstructure fibres provide sufficiently small core diameters for the realisation of this approach. Supercontinua in such fibres can be generated in the regime when multimode-phase-matched four-wave mixing results in a preferable generation of new spectral components emitted as a part of supercontinuum in a certain (perhaps, high-order) guided mode. The results of our experimental studies presented in this paper demonstrate the possibility of separating isolated spatial modes in supercontinuum emission produced in such fibres within different spectral ranges. The proposed method of spatial mode filtering provides a high spatial quality of supercontinuum emission, which is sufficient to allow efficient further frequency conversion of spectrally sliced supercontinuum emission. This frequency convertibility of SC spatial modes was demonstrated by our experiments where spectrally sliced supercontinuum emission was mixed with the fundamental radiation of a Ti:sapphire laser in a nonlinear crystal to produce a sum-frequency signal.

The method of spatial and spectral filtering of supercontinuum emission from microstructure fibres developed in

this paper opens the way to conveniently and efficiently employ MS-fibre-generated supercontinuum emission for spectroscopic applications, time-resolved measurements, optical metrology, and coherence tomography, offering, at the same time, new solutions for synthesising ultrashort light pulses.

Acknowledgements. This study was supported in part by the President of Russian Federation Grant No. 00-15-99304, the Russian Foundation for Basic Research Project No. 00-02-17567, the Volkswagen Foundation Project I/76 869, CRDF Award No. RP2-2266, and the 'Fundamental Metrology' Federal Science and Technology Program of the Russian Federation.

References

1. Ranka J.K., Windeler R.S., Stentz A.J. *Opt. Lett.*, **25**, 25 (2000).
2. Coen St., Chau A.H.L., Leonhardt R., Harvey J.D., Knight J.C., Wadsworth W.J., Russell P.St.J. *Opt. Lett.*, **26**, 1356 (2001).
3. Birks T.A., Wadsworth W.J., Russell P.St.J. *Opt. Lett.*, **25**, 1415 (2000).
4. Holzwarth R., Zimmermann M., Udem Th., Hänsch T.W., Russbuldt P., Gabel K., Poprawe R., Knight J.C., Wadsworth W.J., Russell P.St.J. *Opt. Lett.*, **17**, 1376 (2001).
5. Akimov D.A., Ivanov A.A., Alfimov M.V., Bagayev S.N., Birks T.A., Wadsworth W.J., Russell P.St.J., Fedotov A.B., Pivtsov V.S., Podshivalov A.A., Zheltikov A.M. *Appl. Phys. B*, **74**, 307 (2002).
6. Herrmann J., Griebner U., Zhavoronkov N., Husakou A., Nickel D., Knight J.C., Wadsworth W.J., Russell P.St.J., Korn G. *Phys. Rev. Lett.*, **88**, 173901-1 (2002).
7. Wadsworth W.J., Ortigosa-Blanch A., Knight J.C., Birks T.A., Mann T.P.M., Russell P.St.J. *J. Opt. Soc. Am. B*, **19** (9) (2002).
8. Diddams S.A., Jones D.J., Jun Ye, Cundiff S.T., Hall J.L., Ranka J.K., Windeler R.S., Holzwarth R., Udem T., Hänsch T.W. *Phys. Rev. Lett.*, **84**, 5102 (2000).
9. Holzwarth R., Udem T., Hänsch T.W., Knight J.C., Wadsworth W.J., Russell P.St.J. *Phys. Rev. Lett.*, **85**, 2264 (2000).
10. Bagayev S.N., Dmitriyev A.K., Chepurov S.V., Dychkov A.S., Klementyev V.M., Kolker D.B., Kuznetsov S.A., Matyugin Yu.A., Okhapkin M.V., Pivtsov V.S., Skvortsov M.N., Zakhar'yash V.F., Birks T.A., Wadsworth W.J., Russell P.St.J., Zheltikov A.M. *Laser Phys.*, **11**, 1270 (2001).
11. Hartl I., Li X.D., Chudoba C., Rhanta R.K., Ko T.H., Fujimoto J.G., Ranka J.K., Windeler R.S. *Opt. Lett.*, **26**, 608 (2001).
12. Husakou A.V., Herrmann J. *Phys. Rev. Lett.*, **87**, 203901-1 (2001).
13. Fedotov A.B., Zheltikov A.M., Tarasevitch A.P., von der Linde D. *Appl. Phys. B*, **73**, 181 (2001).
14. Knight J.C., Arriaga J., Birks T.A., Ortigosa-Blanch A., Wadsworth W.J., Russell P.St.J. *IEEE Phot. Technol. Lett.*, **12**, 807 (2000).
15. Knight J.C., Birks T.A., Russell P.St.J., Atkin D.M. *Opt. Lett.*, **21**, 1547 (1996).
16. Fedotov A.B., Alfimov M.V., Ivanov A.A., Tarasishin A.V., Beloglazov V.I., Tarasevitch A.P., von der Linde D., Kirillov B.A., Magnitskii S.A., Chorvat D., Chorvat D. Jr., Naumov A.N., Vlasova E.A., Sidorov-Biryukov D.A., Podshivalov A.A., Kolevatova O.A., Mel'nikov L.A., Akimov D.A., Makarov V.A., Skibina Yu.S., Zheltikov A.M. *Laser Phys.*, **11**, 138 (2001).
17. Zheltikov A.M., Ping Zhou, Temnov V.V., Kondrat'ev Yu.N., Bagayev S.N., Shevandin V.S., Dukel'skii K.V., Khokhlov A.V., Smirnov V.B., Tarasevitch A.P., von der Linde D. *Kvantovaya Elektron.*, **32**, 542 (2002) [*Quantum Electron.*, **32**, 542 (2002)].
18. Fedotov A.B., Konorov S.O., Kondrat'ev Yu.N., Bagayev S.N., Shevandin V.S., Dukel'skii K.V., Sidorov-Biryukov D.A., Khokhlov A.V., Smirnov V.B., Zheltikov A.M. *Laser Phys.* (2002) (in press).